JCN Open Access ORIGINAL ARTICLE
pISSN 1738-6586 / eISSN 2005-5013 / J Clin Neurol 2025;21(5):433-438 / https://doi.org/10.3988/jcn.2025.0199

Comparing Lesion Volume Dynamics Between Multiple Sclerosis and Neuromyelitis Optica Spectrum Disorder During Remission Using Machine-Learning Segmentation

Shaun G. Hong[a,b*]
Ki Hoon Kim[b,c*]
You-Ri Kang[b,d]
Jae-Won Hyun[b]
Su-Hyun Kim[b]
Ho Jin Kim[b]

[a]Weldon School of Biomedical Engineering, Purdue University, West Lafayette, IN, USA
[b]Department of Neurology, Research Institute and Hospital of National Cancer Center, Goyang, Korea
[c]Department of Neurology, Severance Hospital, Yonsei University College of Medicine, Seoul, Korea
[d]Department of Neurology, Chonnam National University Hospital, Gwangju, Korea

Background and Purpose Multiple sclerosis (MS) and neuromyelitis optica spectrum disorder (NMOSD) are inflammatory demyelinating conditions of the central nervous system that have distinct pathological mechanisms. There is a paucity of studies comparing the accumulation of subclinical lesions between MS and NMOSD, especially during the clinical remission period. Recent advances in neuroimaging techniques, those particularly involving the use of machine learning (ML) methods for lesion segmentation, have provided new opportunities to quantitatively assess the volumes of brain lesions and how they change over time. In this study, we aimed to use ML-based lesion segmentation methods to measure differences in lesion volumes and their changes during the remission period between patients with MS and NMOSD.

Methods This study included a retrospective cohort of 31 patients with MS and patients with 30 aquaporin-4-positive (AQP4$^+$) NMOSD from the National Cancer Center registry. Serial 3D brain magnetic resonance imaging (MRI) scans obtained during the interattack period were analyzed using ML-based segmentation. MRI data preprocessing included alignment, distortion correction, and normalization, with lesion mapping and statistical analyses determining changes in lesion volumes.

Results The MS patients exhibited significant increases in the median lesion volume (from 3,493 mm^3 to 4,430 mm^3, p<0.001), indicating ongoing subclinical activity without clinical relapses. In contrast, the NMOSD patients showed no significant change in the median lesion volume (from 640 mm^3 to 930 mm^3, p=0.129), supporting an attack-dependent disease course. The lesion volume increased by 193 mm^3/year in the MS group, compared with only 25 mm^3/year in the NMOSD group (p=0.017).

Conclusions These findings highlight the distinct pathogenic processes of the two conditions and hence the need for specialized therapeutic and monitoring strategies for patients with MS and AQP4$^+$ NMOSD.

Keywords multiple sclerosis; subclinical activity; neuromyelitis optica spectrum disorder; machine learning.

Received April 19, 2025
Revised June 3, 2025
Accepted June 8, 2025

Correspondence
Ho Jin Kim, MD, PhD
Department of Neurology, Research Institute and Hospital of National Cancer Center, 323 Ilsan-ro, Ilsandong-gu, Goyang 10408, Korea
Tel +82-31-920-2438
Fax +82-31-905-5524
E-mail hojinkim@ncc.re.kr

*These authors contributed equally to this work.

INTRODUCTION

Multiple sclerosis (MS) and neuromyelitis optica spectrum disorder (NMOSD) are inflammatory demyelinating conditions of the central nervous system (CNS) that have distinct pathological mechanisms.[1,2] The development of subclinical demyelinating lesions is a recognized characteristic of MS. These lesions can develop asymptomatically, independent of clinical attacks,[3] and contribute to the gradual accumulation of neurological deficits and disability. Meanwhile, NMOSD is thought to be an attack-dependent disease, with the development of subclinical lesions being rare.[4,5]

There is a paucity of studies directly comparing the accumulation of subclinical lesions between MS and NMOSD, especially during the clinical remission period. It is crucial to address this knowledge gap since understanding the differences in lesion behavior between these two conditions could have important implications for disease monitoring and treatment strategies. Recent advances in neuroimaging techniques, particularly those involving the use of machine learning (ML) methods for lesion segmentation, have provided new opportunities to quantitatively assess the volumes of brain lesion and how they change over time.[6] These methods offer improved accuracy and reproducibility compared with traditional techniques.

In this study, we aimed to measure differences in brain lesion volumes and their changes during the clinical remission period between patients with MS and NMOSD. We hoped that applying ML-based lesion segmentation methods would provide a more-detailed understanding of the subclinical disease activities in these two conditions.

METHODS

Participants

This retrospective cohort study reviewed the medical records and brain magnetic resonance imaging (MRI) data of 31 patients with MS and 30 patients with aquaporin-4-positive ($AQP4^+$) NMOSD from the National Cancer Center (NCC) registry. The inclusion criteria for participants were 1) adult patients aged 18 years or older diagnosed with relapsing–remitting MS according to the 2017 McDonald criteria,[7] or the 2015 diagnostic criteria for $AQP4^+$ NMOSD verified through live cell-based assays[8]; 2) availability of comprehensive demographic and clinical data from throughout the disease course; 3) availability of serial brain 3D MRI scans obtained during the interattack period (>3 months from the clinical attack) with an interval of at least 6 months; and 4) absence of clinical attacks between paired MRI scans. Demographic data were also collected, including on sex, age at disease onset, and type of disease-modifying therapy (DMT).

MRI equipment and parameters

Imaging was conducted using a 3.0-tesla scanner (Philips Achieva, Philips Medical Systems) incorporating a 32-channel phased-array receiver head coil. Whole-brain images were obtained to ensure that intracranial structures and lesions were captured comprehensively. Structural imaging sequences including T1-weighted and T2-weighted fluid-attenuated inversion-recovery (FLAIR) modalities where obtained using a flip angle of 9°, 208 slices, and an isotropic voxel size of 1.0×1.0 mm^3.

Preprocessing workflow

MRI data preprocessing included steps for alignment, distortion correction, outlier identification, and normalization. Realignment was performing using the realign and unwarp procedure of Statistical Parametric Mapping (SPM) software[9] to align all scans to the initial image obtained during the first imaging session using a least-squares optimization and rigid-body transformation.[10] Resampling utilized b-spline interpolation to account for motion artifacts and susceptibility distortions. Temporal inconsistencies during the acquisition of interleaved slices were corrected by applying sinc temporal interpolation.[11,12] Artifact detection tools were used to identify outlier frames exhibiting displacements exceeding 0.9 mm or global signals deviating by more than five standard deviations (SDs). A reference image was generated by averaging all scans excluding the detected outliers,[13,14] and then the data were normalized using the unified segmentation and normalization framework of the SPM software to map images onto the standard Montreal Neurological Institute space and segment them into gray matter, white matter, and cerebrospinal fluid (CSF) tissue. Resampling to a 2-mm isotropic voxel resolution was performed using the IXI-549 tissue probability map template.[15-17] The processed data underwent spatial smoothing with an 8-mm full-width-at-half-maximum Gaussian kernel.

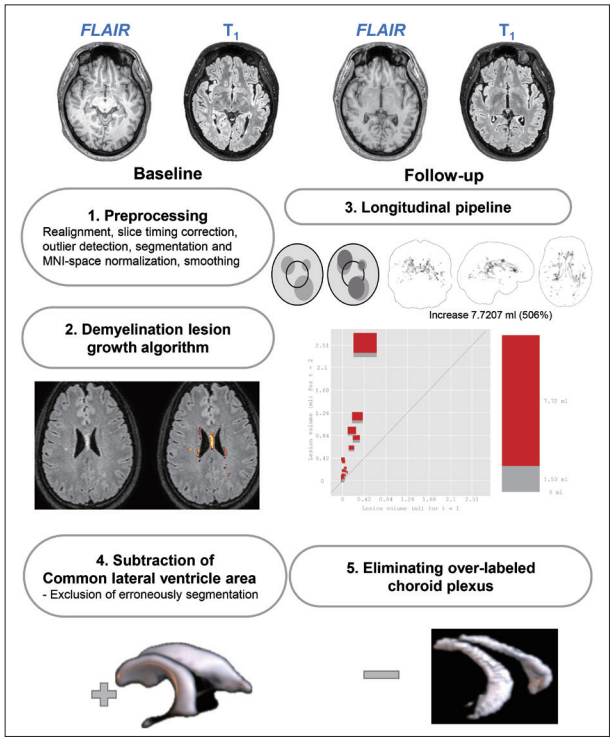

Fig. 1. Flowchart of the image analysis process. FLAIR, fluid-attenuated inversion-recovery.

Image processing

Lesion segmentation was performed using version 3.0.0 of the SPM Lesion Segmentation Toolbox (LST), which applies a lesion-growth algorithm to both T1-weighted and FLAIR images. This algorithm has been validated in previous studies showing strong correlations with manual segmentations in MS cohorts.[18,19]

Binary lesion maps for individual subjects were created that were normalized to a common spatial framework using transformations derived from corresponding T1-weighted images, and filled with lesion data prior to normalization. These maps were subsequently aggregated to produce a joint normalized lesion map while ensuring there were no voxel overlaps across subjects. This approach facilitated the exclusion of erroneously segmented choroid plexus regions. False-positive segmentations were minimized by using a subtraction method to exclude erroneously segmented choroid plexus regions and CSF-filled spaces, including the lateral ventricle area. A flowchart of the image analysis process is shown in Fig. 1.

Statistical analyses

Mean±SD, median and interquartile range (IQR), or number and percentage values were calculated for each dataset. Lesion volume changes were compared between groups using the Mann–Whitney U test due to the data not conforming to a normal distribution. The Wilcoxon signed-rank test or McNemar test was used to quantify changes in lesion volumes between paired brain MRI scans. Group differences in lesion volume changes were evaluated using multiple linear regression analysis while adjusting for age, sex, and MRI-scan interval. To account for variations in the intervals between paired MRI scans, the annualized lesion volume change was calculated as the absolute difference in lesion volume divided by the time interval in years. Additionally, a post-hoc power analysis was conducted using G*Power software (version 3.1.9.7, Heinrich Heine University) to evaluate the adequacy of the sample size. The analysis employed SPM (RRID: SCR_007037, version 12.7771) alongside an automated lesion-growth-based segmentation algorithm (RRID: 3.0.0) for demyelination. GraphPad Prism (version 10.3, GraphPad Software, LLC) and R software (version 4.3.2, R Foundation for Statistical Computing) were used for the data analyses and visualization. The protocol of this study was approved by the Institutional Review Board of the NCC (NCC2014 -0146). Informed consent was not required due to the use of anonymized data.

Table 1. Characteristics of the enrolled patients, and inflammatory lesion volumes

	Patients with MS (*n*=31)		Patients with NMOSD (*n*=30)	*p*
Sex, female	25 (81)		26 (87)	n.s.
Age at onset (yr)	24.1±7.8		34.5±11.0	0.004
Age at first MRI scan (yr)	28.5±8.1		39.7±9.2	<0.001
Time interval between paired MRI scans (month)	26.3 [19.8 to 35.6]		39.8 [35.5 to 41.36]	<0.001
Treatment at the time of the first MRI scan				
Interferon-beta	10 (32)	Azathioprine	2 (7)	
Dimethyl fumarate	5 (16)	Mycophenolate mofetil	5 (17)	
Glatiramer acetate	3 (10)	Rituximab	23 (77)	
Natalizumab	3 (10)			
Teriflunomide	2 (6)			
Cladribine	2 (6)			
Fingolimod	1 (3)			
Rituximab	1 (3)			
None	4 (13)			
Volume of inflammatory lesions (mm^3)				
Baseline	3,493 [983 to 7,550]		640 [65 to 1,895]	<0.001
Follow-up	4,430 [1,611 to 9,673]		930 [88 to 2,068]	<0.001
Volume change between baseline and follow-up	563 [-55 to 1,886]		84 [-65 to 604]	0.042
Annualized volume change	193 [-27 to 994]		25 [-33 to 183]	0.017

Data are mean±SD, median [IQR], or *n* (%) values.
IQR, interquartile range; MRI, magnetic resonance imaging; MS, multiple sclerosis; NMOSD, neuromyelitis optica spectrum disorder; n.s., not significant; SD, standard deviation.

RESULTS

Table 1 summarizes the demographic and clinical data and the inflammatory lesion volumes of the enrolled patients. The patients were predominantly female, comprising 81% and 87% of those in the MS and NMOSD groups, respectively. The age at disease onset was lower in the MS group than the NMOSD group (24.1±7.8 years vs. 34.5±11.0 years, p=0.004), while the median time interval between paired MRI scans was significantly longer in the NMOSD group (39.8 months, IQR=35.5–41.36 months) than the MS group (26.3 months, IQR=19.8–35.6 months, p<0.001). The observed effect size (Cohen's d=0.82) yielded a post-hoc statistical power of 0.88, indicating that the sample size was sufficient for detecting between-group differences.

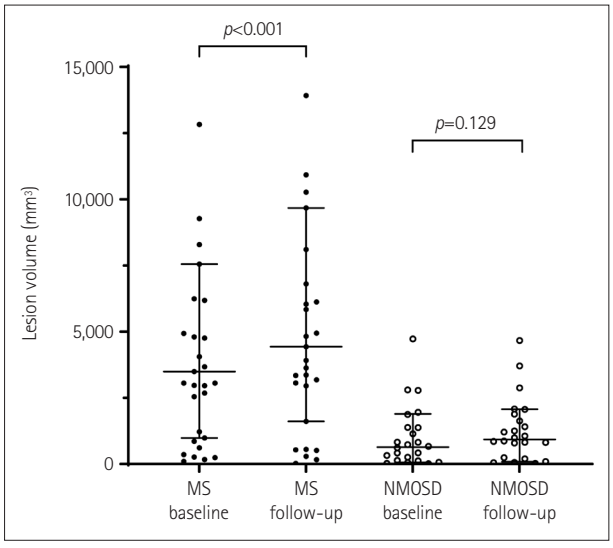

Fig. 2. Comparison of lesion volumes between MS and NMOSD patients. The median inflammatory lesion volume was higher in the MS group (3,493 mm^3) than the NMOSD group (640 mm^3, p<0.001). Follow-up MRI scans showed that the lesion volume increased significantly in the MS group (p<0.001) but not in the NMOSD group (p=0.129). MRI, magnetic resonance imaging; MS, multiple sclerosis; NMOSD, neuromyelitis optica spectrum disorder.

Fig. 2 displays the lesion volumes in the MS and NMOSD groups, as well as their changes observed in the follow-up MRI scans. At baseline, the median inflammatory lesion volume was higher in the MS group (3,493 mm^3, IQR=983–7,550 mm^3) than the NMOSD group (640 mm^3, IQR=65–1,895 mm^3, p<0.001). In follow-up MRI scans the median lesion volume had increased in the MS group to 4,430 mm^3 (IQR=1,611–9,673 mm^3, p<0.001), while it had not changed significantly in the NMOSD group (p=0.129). Even though the time interval between paired MRI scans was longer in the NMOSD group, the median lesion volume increased more in the MS group (+563 mm^3 vs. +84 mm^3, p=0.042). After adjusting for age, sex, and MRI-scan interval, the difference in the increase in lesion volume between the MS and NMOSD groups remained statistically significant (p=0.014). The median intergroup difference was more pronounced for the annualized volume change of inflammatory lesions, being +193 mm^3 in the MS group and +25 mm^3 in the NMOSD group (p=0.017). These findings are presented in Fig. 3, while Supplementary Fig. 1 (in the online-only Data Supplement) additionally illustrates the individual lesion-volume trajectories for both groups.

DISCUSSION

This study used ML-based lesion segmentation to reveal that MS and AQP4$^+$ NMOSD patients show distinct differences in brain lesion volumes and their dynamics during the re-

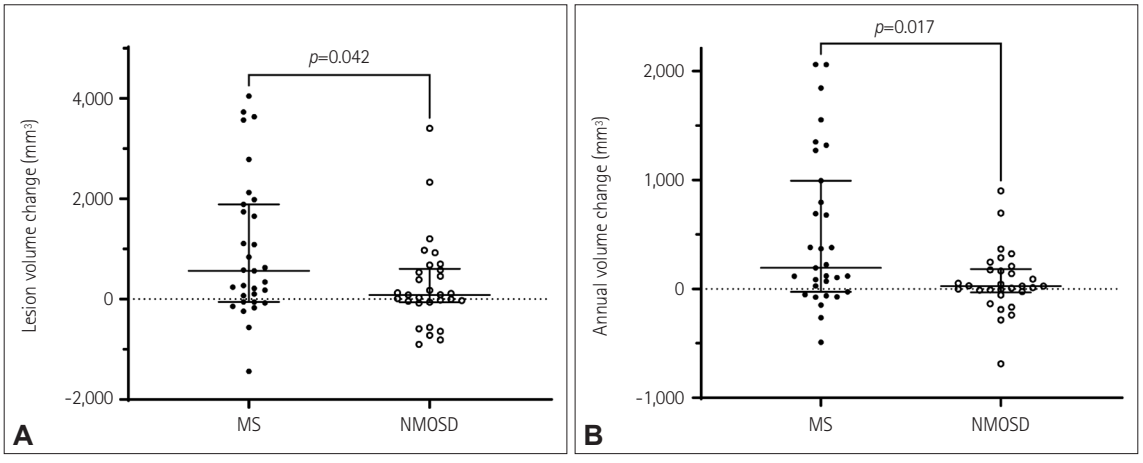

Fig. 3. Comparison of subclinical lesion changes between MS and NMOSD patients. A: The median increase in lesion volume was larger in the MS group (+563 mm^3) than the NMOSD group (+84 mm^3, p=0.042). B: The annualized change in inflammatory lesion volume was also significantly larger in the MS group (+193 mm^3) than the NMOSD group (+25 mm^3, p=0.017). MS, multiple sclerosis; NMOSD, neuromyelitis optica spectrum disorder.

mission period. Inflammatory brain lesions are larger and exhibit larger annualized changes in MS patients than in AQP4+ NMOSD patients, suggesting the presence of subclinical disease progression in MS, whereas such progression appears unlikely in NMOSD. These findings highlight the distinct pathogenic processes of the two conditions and the need for specialized therapeutic and monitoring strategies for patients with MS and AQP4+ NMOSD.

The distinct immunopathological profiles of MS and NMOSD provide a framework for interpreting these findings. The progression of MS is thought to result from dynamic interactions between peripheral immune activation and compartmentalized inflammation within the CNS.[20] Chronic immune processes become increasingly trapped within the CNS over time, contributing to sustained demyelination, axonal degeneration, and neurodegeneration. Meningeal inflammation, including ectopic lymphoid follicles composed of B cells and T cells, plays a critical role in maintaining this chronic immune response. These mechanisms can explain the silent progression in MS, independently of clinical relapses or radiological activity.[20,21] In contrast, NMOSD is primarily driven by a peripheral, humoral immune response that is largely mediated by AQP4-IgG and complement activation, which are closely associated with clinical relapses and do not typically result in subclinical CNS lesion accumulation.[1,22]

ML-based lesion segmentation has emerged as a powerful tool in neuroimaging that offers several advantages over traditional manual and semiautomated approaches. In contrast with conventional segmentation methods being labor-intensive and prone to variability, ML techniques leverage data-driven feature extraction to improve accuracy, consistency, and reproducibility. Recent studies have shown that segmentation performed using deep-learning models (particularly convolutional neural networks) significantly improves the sensitivity and specificity in detecting lesions compared with using traditional techniques, and facilitates automated lesion tracking and the monitoring of disease progression in MS.[18,23,24] While ML-based segmentation in NMOSD has been studied less extensively, recent applications of deep learning have produced promising results in differentiating NMOSD lesions from MS.[25,26]

Building on previous research, the present study focused on silent lesion accumulation during the remission period, directly comparing inflammatory lesion volumes and their annualized changes in MS and NMOSD. Our results support the continuous accrual of clinically silent lesions in MS that could contribute to progressive neurological decline.[27] Thus, even in clinically stable MS, performing brain follow-up MRI scans annually should be regarded as routine care since it enables the detection of subclinical disease activity and thereby facilitates timely adjustments in DMT strategies.[28,29] In contrast, the minimal changes in lesion volumes during remission in NMOSD suggest employing a different monitoring strategy from that in MS. Previous research has also indicated that disability progression in NMOSD primarily occurs during clinical attacks,[30,31] and asymptomatic brain lesions are seldom detected on MRI in clinically stable patients with NMOSD.[4] The attack-dependent nature of NMOSD suggests that regular MRI monitoring would be of little value in managing this condition.

This study had several limitations. Firstly, its retrospective design and relatively small sample may have reduced the generalizability of the findings. Secondly, while a validated and widely used tool (LST) was used for automated lesion quantification, we were not able to perform direct validation with manual segmentation for this dataset. However, it has previously been demonstrated that the LST provided good agreement with manual segmentation in MS cohorts, and we incorporated several postprocessing steps, including removing nonparenchymal structures and performing spatial normalization onto a standard anatomical space. Thirdly, although lesion volume changes were annualized, variability in the follow-up intervals may have adversely affected the comparisons of lesion dynamics, and this should be considered when interpreting the findings. Notwithstanding these limitations, this study is the first to compare inflammatory lesion volumes and their changes using an ML-based segmentation method between MS and NMOSD, and has revealed their distinct pathogenic characteristics and the need for specialized therapeutic and monitoring strategies.

Supplementary Materials

The online-only Data Supplement is available with this article at https://doi.org/10.3988/jcn.2025.0199.

Availability of Data and Material

The datasets generated or analyzed during the study are available from the corresponding author on reasonable request.

ORCID iDs

Shaun G. Hong https://orcid.org/0000-0003-3265-7325
Ki Hoon Kim https://orcid.org/0000-0001-6428-061X
You-Ri Kang https://orcid.org/0000-0001-5189-1323
Jae-Won Hyun https://orcid.org/0000-0003-0288-771X
Su-Hyun Kim https://orcid.org/0000-0002-0679-0918
Ho Jin Kim https://orcid.org/0000-0002-8672-8419

Author Contributions

Conceptualization: Shaun G. Hong, Ki Hoon Kim, Ho Jin Kim. Funding acquisition: Ki Hoon Kim. Resources: all authors. Supervision: Ho Jin Kim. Visualization: Shaun G. Hong, Ki Hoon Kim. Writing—original draft: Shaun G. Hong, Ki Hoon Kim. Writing—review & editing: all authors.

Conflicts of Interest

SG Hong and Y-R Kang report no disclosures.
KH Kim has received a grant from the Korean Society of Neuroimmunology.
S-H Kim has lectured, consulted, and received honoraria from Bayer Schering Pharma, Biogen, Genzyme, Merck Serono, and UCB and received a grant from the National Research Foundation of Korea.
J-W Hyun has received a grant from the National Cancer Center in Korea.
HJ Kim received a grant from the National Research Foundation of Korea and research support from AprilBio, Eisai, Good T cells and UCB; received consultancy/speaker fees from Alexion, Altos Biologics, AstraZeneca, Biogen, Daewoong Pharmaceutical, Eisai, GC Pharma, Handok Pharmaceutical, Kaigene, Kolon Life Science, MDimune, Merck, Mitsubishi Tanabe Pharma, Roche, and Sanofi; is a co-editor for the Multiple Sclerosis Journal and an associated editor for the Journal of Clinical Neurology.

Funding Statement

This work was supported by the Korean Society of Neuroimmunology.

REFERENCES

1. Jarius S, Paul F, Weinshenker BG, Levy M, Kim HJ, Wildemann B. Neuromyelitis optica. *Nat Rev Dis Primers* 2020;6:85.
2. Filippi M, Bar-Or A, Piehl F, Preziosa P, Solari A, Vukusic S, et al. Multiple sclerosis. *Nat Rev Dis Primers* 2018;4:43.
3. Min M, Spelman T, Lugaresi A, Boz C, Spitaleri D, Pucci E, et al. Silent lesions on MRI imaging - shifting goal posts for treatment decisions in multiple sclerosis. *Mult Scler* 2018;24:1569-1577.
4. Lee MY, Yong KP, Hyun JW, Kim SH, Lee SH, Kim HJ. Incidence of interattack asymptomatic brain lesions in NMO spectrum disorder. *Neurology* 2020;95:e3124-e3128.
5. Camera V, Holm-Mercer L, Ali AAH, Messina S, Horvat T, Kuker W, et al. Frequency of new silent MRI lesions in myelin oligodendrocyte glycoprotein antibody disease and aquaporin-4 antibody neuromyelitis optica spectrum disorder. *JAMA Netw Open* 2021;4:e2137833.
6. Zeng C, Gu L, Liu Z, Zhao S. Review of deep learning approaches for the segmentation of multiple sclerosis lesions on brain MRI. *Front Neuroinform* 2020;14:610967.
7. Thompson AJ, Banwell BL, Barkhof F, Carroll WM, Coetzee T, Comi G, et al. Diagnosis of multiple sclerosis: 2017 revisions of the McDonald criteria. *Lancet Neurol* 2018;17:162-173.
8. Wingerchuk DM, Banwell B, Bennett JL, Cabre P, Carroll W, Chitnis T, et al. International consensus diagnostic criteria for neuromyelitis optica spectrum disorders. *Neurology* 2015;85:177-189.
9. Andersson JL, Hutton C, Ashburner J, Turner R, Friston K. Modeling geometric deformations in EPI time series. *Neuroimage* 2001;13:903-919.
10. Friston KJ, Ashburner J, Frith CD, Poline JB, Heather JD, Frackowiak RSJ. Spatial registration and normalization of images. *Hum Brain Map* 1995;3:165-189.
11. Henson R, Büchel C, Josephs O, Friston K. The slice-timing problem in event-related fMRI. *Neuroimage* 1999;9:125.
12. Sladky R, Friston KJ, Tröstl J, Cunnington R, Moser E, Windischberger C. Slice-timing effects and their correction in functional MRI. *Neuroimage* 2011;58:588-594.
13. NeuroLmaging Tools & Resources Collaboratory. Artifact detection tools [Internet]. NeuroLmaging Tools & Resources Collaboratory [cited 2025 Jun 23]. Available from: https://www.nitrc.org/projects/artifact_detect/.
14. Power JD, Mitra A, Laumann TO, Snyder AZ, Schlaggar BL, Petersen SE. Methods to detect, characterize, and remove motion artifact in resting state fMRI. *Neuroimage* 2014;84:320-341.
15. Calhoun VD, Wager TD, Krishnan A, Rosch KS, Seymour KE, Nebel MB, et al. The impact of T1 versus EPI spatial normalization templates for fMRI data analyses. *Hum Brain Mapp* 2017;38:5331-5342.
16. Ashburner J. A fast diffeomorphic image registration algorithm. *Neuroimage* 2007;38:95-113.
17. Ashburner J, Friston KJ. Unified segmentation. *Neuroimage* 2005;26:839-851.
18. Duong MT, Rudie JD, Wang J, Xie L, Mohan S, Gee JC, et al. Convolutional neural network for automated FLAIR lesion segmentation on clinical brain MR imaging. *AJNR Am J Neuroradiol* 2019;40:1282-1290.
19. Schmidt P, Gaser C, Arsic M, Buck D, Förschler A, Berthele A, et al. An automated tool for detection of FLAIR-hyperintense white-matter lesions in multiple sclerosis. *Neuroimage* 2012;59:3774-3783.
20. Kuhlmann T, Moccia M, Coetzee T, Cohen JA, Correale J, Graves J, et al. Multiple sclerosis progression: time for a new mechanism-driven framework. *Lancet Neurol* 2023;22:78-88.
21. Klotz L, Antel J, Kuhlmann T. Inflammation in multiple sclerosis: consequences for remyelination and disease progression. *Nat Rev Neurol* 2023;19:305-320.
22. Uzawa A, Oertel FC, Mori M, Paul F, Kuwabara S. NMOSD and MOGAD: an evolving disease spectrum. Nat Rev Neurol 2024;20:602-619.
23. Cho J, Park KS, Karki M, Lee E, Ko S, Kim JK, et al. Improving sensitivity on identification and delineation of intracranial hemorrhage lesion using cascaded deep learning models. *J Digit Imaging* 2019;32:450-461.
24. Daqqaq TS, Alhasan AS, Ghunaim HA. Diagnostic effectiveness of deep learning-based MRI in predicting multiple sclerosis: a meta-analysis. *Neurosciences (Riyadh)* 2024;29:77-89.
25. Seok JM, Cho W, Chung YH, Ju H, Kim ST, Seong JK, et al. Differentiation between multiple sclerosis and neuromyelitis optica spectrum disorder using a deep learning model. *Sci Rep* 2023;13:11625.
26. Kim H, Lee Y, Kim YH, Lim YM, Lee JS, Woo J, et al. Deep learning-based method to differentiate neuromyelitis optica spectrum disorder from multiple sclerosis. *Front Neurol* 2020;11:599042.
27. Sormani MP, Bruzzi P. MRI lesions as a surrogate for relapses in multiple sclerosis: a meta-analysis of randomised trials. *Lancet Neurol* 2013;12:669-676.
28. Wattjes MP, Ciccarelli O, Reich DS, Banwell B, de Stefano N, Enzinger C, et al. 2021 MAGNIMS-CMSC-NAIMS consensus recommendations on the use of MRI in patients with multiple sclerosis. *Lancet Neurol* 2021;20:653-670.
29. McGinley MP, Goldschmidt CH, Rae-Grant AD. Diagnosis and treatment of multiple sclerosis: a review. *JAMA* 2021;325:765-779.
30. Siriratnam P, Huda S, Van Der Walt A, Sanfilippo PG, Sharmin S, Foong YC, et al. Prevalence of progression independent of relapse activity and relapse-associated worsening in patients with AQP4-IgG-positive NMOSD. *Neurology* 2024;103:e209940.
31. Akaishi T, Takahashi T, Misu T, Abe M, Ishii T, Fujimori J, et al. Progressive patterns of neurological disability in multiple sclerosis and neuromyelitis optica spectrum disorders. *Sci Rep* 2020;10:13890.